Article

Not peer-reviewed version

Green Synthesis of CuO Nanoparticles from Macroalgae *Ulva lactuca* and *Gracilaria verrucosa*

Marta Marmiroli * , Marco Villani , Paolina Scarponi , Silvia Carlo , Luca Pagano , Valentina Sinisi , Laura Lazzarini , Milica Pavlicevic , Nelson Marmiroli

Posted Date: 12 June 2024

doi: 10.20944/preprints202406.0774.v1

Keywords: Green Macroalgae; Red Macroalgae; CuO NPs; Bactericidal; Fungicidal

 doi:10.20944/preprints202406.0774.v1

Article

Green Synthesis of CuO Nanoparticles from Macroalgae *Ulva lactuca* and *Gracilaria verrucosa*

Marta Marmiroli [1,*], Marco Villani [2], Paolina Scarponi [1], Silvia Carlo [1], Luca Pagano [3], Valentina Sinisi [2], Laura Lazzarini [2], Milica Pavlicevic [1] and Nelson Marmiroli [3]

[1] Dept. Chemistry, Life Sciences, and Environmental Sustainability, University of Parma, Parco Area delle Scienze, 43124, Parma, Italy
[2] CNR IMEM, Parco Area delle Scienze, 43124, Parma, Italy
[3] Consorzio Interuniversitario Nazionale per le Scienze Ambientali (CINSA), University of Parma, Parco Area delle Scienze, 43124, Parma, Italy.
* Correspondence: author. E-mail: marta.marmiroli@unipr.it

Abstract: Macroalgae seaweeds such as *Ulva lactuca* and *Gracilaria verrucosa* cause problems on the Northern Coast of the Italian Adriatic Sea because their overabundance hinders the growth of cultivated clams, *Rudatapes philippinarum*. This study focused on the green synthesis of CuO nanoparticles from *U. lactuca* and *G. verrucosa*. The biosynthesized CuO NPs were successfully characterized using FTIR, XRD, HRTEM/EDX, and zeta potential. Nanoparticles from the two different algae species are essentially identical, with the same physical characteristics and almost the same antimicrobial activities. We have not investigated the cause of this identity, but it seems likely to arise from the reaction of Cu with the same algae metabolites in both species. The study demonstrates that it is possible to obtain useful products from these macroalgae through a green synthesis approach and that they should be considered as not just a cause of environmental and economic damage but also as a potential source of income.

Keywords: Green Macroalgae; Red Macroalgae; CuO nanoparticles; bactericidal; fungicidal

1. Introduction

Nanotechnology can blend the principles of biology with physical and chemical sciences to generate nano-sized particles having specific functions (Gnanajobitha, et al., 2013. Suresh, et al., 2011. Kumar, et al., 2014. Mariselvam, et al., 2014). Nanoparticles (NPs) exhibit different sizes and shapes but diameters are typically between 1 nm and 100 nm. Compared to the bulk material, NPs have unique physicochemical properties due to their high surface area to volume ratio. Reduced cohesive energy (especially of the surface atoms at sharp corners and edges, which become very reactive), and a higher degree of curvature, enable NPs to act as catalysts for surface-sensitive reactions (Jin et al., 2012).

Such remarkable characteristics give rise to novel opportunities in different fields including therapeutics, optoelectronics, drug discovery, diagnostic biological probes, catalysis, display instruments, biological sensors, and detection of environmental toxic metals or other contaminants (Pearce et al., 2021; Mourdikoudis, et al. 2018; Zhao. et al., 2018). Most nanoparticles are prepared by inorganic synthesis, but it is also possible to synthesize them utilizing natural products such as plants and algae, and bacterial and fungal extracts (El-Seedi et al. 2019).

NPs can be synthesized by two fundamental approaches: top-down and bottom-up. Within the top-down approach, NPs are generated by reducing the size of their bulk counterpart employing several physical and chemical methods (Singh, et al. 2010) including microfabrication techniques, where external tools are applied to precisely cut, mill, or otherwise change the material into a desired size and structure (Khan, et al. 2019; Nath et al. 2013). These microfabrication techniques include laser

 doi:10.20944/preprints202406.0774.v1

ablation, etching, sputtering, mechanical milling, and electro-explosion (Abid et al., 2022; Priyadarshana et al. 2015).

The bottom-up approach produces NPs by the assembly of atoms, molecules, and clusters. Hence, it is also referred to as "molecular nanotechnology" (Abid et al., 2022; Thakkar, et al. 2010). The nano-sized structures produced by the bottom-up approach are created by methods such as chemical reduction, plasma or flame spraying, sol-gel processes, molecular condensation, supercritical fluid synthesis, laser pyrolysis, use of templates, chemical vapor deposition and, most significantly, by alternative biologically-based green synthesis (Türk et al. 2018; Sangeetha et al. 2014; Chatterjee et al. 2020).

Compared to chemical methods, biological materials are in high demand for NPs synthesis. A wide variety of marine and freshwater algae, plants, bacteria, actinomycetes, fungi, viruses, and yeasts have been utilized for NP synthesis because they are eco-friendly and inexpensive; these processes are called "nanobiofactories". These living entities vary in their biochemical processing potential, which can be utilized for the synthesis of metallic oxide and metallic NPs (Zulfiqar et al., 2019).

Macroalgae (seaweeds) are often used as a potential source of secondary metabolites, including phenolic compounds, pigments, and polysaccharides (Ficko-Blean et al., 2015). Biosynthesis based on the abilities of macroalgae as nanobiofactories targets algal secondary metabolites for use as reducing agents to stabilize NPs; most studies have been focused on the production from algae of metal (Ag, Au) and metal-oxide (CuO, ZnO) NPs: the eco-friendly biosynthesis of metal NPs using bioactive compounds from macroalgae reduces cost and production time and increases their biocompatibility, making them suitable for a wide variety of applications (Hu et al., 2007; Barciela et al., 2023).

Marine algae contain sulfated polysaccharides (Ficko-Blean et al., 2015). The main cell wall components of brown macroalgae, for example, are anionic polysaccharides including alginates and fucose-containing sulfated polysaccharides. Red macroalgae extracellular matrices (ECMs) contain sulfated galactans, agars, and carrageenans. In comparison, marine green macroalgae ECMs include four types of polysaccharides: semicrystalline cellulose, water-soluble ulvans, and two minor hemicelluloses: a xyloglucan and a glucuronan (Ray et al., 1995). Seaweeds also contain pharmacologically active substances such as alkaloids, flavonoids, terpenoids, and phenols. Marine brown, red, and green macroalgae have significant differences in their physiological and intracellular biological contents. A comprehensive description of the constituents of brown, red, and green macroalgae is reported by Kloareg et al. (2021).

These properties and their abundance as a raw material have attracted many researchers to consider their use in cleaner methods for NPs synthesis (Castro, et al., 2013). There is a recent trend in nanotechnology to evaluate possible synergic effects between the nanomaterials being produced and natural biomolecules. Among these, natural antioxidants have attracted considerable attention since they can act against oxidative stress, which has been shown to be an important factor in the appearance and evolution of many morbidity processes, such as diabetes, cardiovascular diseases, cancer, Parkinson's and Alzheimer's diseases, arthritis, and even aging (Khalil, 2020). Algae are photoautotrophic and produce much of the world's oxygen. They can also bioaccumulate heavy metals. Antimicrobial activity is a desired property of new biological synthesized nanomaterials. Seaweeds can potentially reduce oxide materials to antibacterial metallic nanoparticles: the first metallic nanoparticles, with their unique antibacterial properties, were produced using *Sargassum weightii* (Singaravelu et al., 2007).

Very little research has been conducted on the biological impact of green-synthesized NPs. Studies on nanoparticle toxicity, uptake mechanisms, and bioaccumulation are required. Compared with chemically synthesized NPs, green-synthesized NPs are not widely used in industry. Antimicrobial resistance is one of the ten major global public threats facing humanity and is considered by the World Health Organization as a priority issue (WHO, 2021, EClinicalMedicine, 2021). Bacterial and fungal infections of humans are common worldwide, and treatment is becoming increasingly challenging due to increasing resistance to standard antimicrobials. Biofilm-forming bacteria are recognized as a bigger threat, as biofilm-residing cells can be impervious to the host's

 doi:10.20944/preprints202406.0774.v1

immune system, antibiotics, and other treatments (Vestby et al., 2020). Among the nineteen pathogens identified as priorities by the World Health Organization (WHO) in its first Fungal Priority Pathogens List—WHO FPPL, published in 2022—*C. albicans* and *C. auris* are placed in the critical priority group (WHO, 2022; De Oliveira et al., 2020). *C. albicans* can rapidly acquire resistance to the most frequently used antifungals, such as fluconazole. The exponential development in recent years of multidrug resistance, combined with the scarcity of novel antifungal drugs due to the difficulty in ensuring selectivity in relation to animal cells, has propelled research on metal nanoparticles as potential alternatives (Mussin et al., 2022). Similarly, the bacteria *Escherichia coli, Pseudomonas aeruginosa,* and *Staphylococcus aureus* are among the most challenging antibiotic-resistant pathogens (Pereira et al., 2021). These opportunistic and nosocomial pathogens are associated with high rates of mortality and impose a great economic burden on society.

One of the algae that we have used in our work is *G. verrucosa*, common in the Mediterranean area and the Northern Adriatic Sea. *G. veruccosa* is a red seaweed primarily distributed along the coastal regions of Tamil Nadu, India (Mantri et al., 2019). It is known to have antibacterial, antifungal, and antihemolytic properties (De Almeida et al., 2011). Gold nanoparticles green-synthesized using *G. veruccosa* are biocompatible with normal human embryonic cells (HEK-293) (Chellapandian et al., 2019). However, reports are rare of the green synthesis of CuO NPs. The other seaweed that we have used is *Ulva lactuca*, also common to the Northern Adriatic Sea, and other temperate coasts. Its biomass contains a large amount of the polysaccharide ulvan, together with carotenoids and phenolics, lipids and proteins, and it has abundant antioxidant activity (Pappou et al., 2022).

The shallow lagoons of the Northern Adriatic Sea, including Sacca di Goro, are the most important sites within the European Community for cultivation of the Manila clam (*Rudatapes philippinarum*) with a crop estimated at between 50 000 and 60 000 t y^{-1}. Clam farming in Sacca di Goro is managed, mostly in a sustainable way, by cooperatives of fishermen that exploit licensed areas, under the control of regional and local authorities (Zaldívar et al., 2003). In recent years, clam farming has suffered serious setbacks due to massive clam mortality in summer. Uncontrolled growth of the seaweeds and the occurrence of dystrophic events triggered by decomposition of macroalgal biomass have been proposed as major factors causing the decline of clam farming in the lagoon (Viaroli et al., 2001). For these reasons, the macroalgae are considered as waste and a noxious byproduct to be disposed of.

The purpose of this work was to produce useful nanoparticles from these macroalgae to reverse their role from a problem to a resource. In particular, we focused on obtaining CuO nanoparticles from an extract of the red and green macroalgae. The nanoparticles were tested on pathogenic and non-pathogenic microorganisms to determine if they have antimicrobial properties.

2. Results and Discussion

2.1. Green Synthesis of CuO Nanoparticles from Macroalgae

The copper acetate solution used for NPs synthesis had initial and final pHs of 6.1 and 5.2, and 6.3 and 5.1 respectively for the green algae (GA) and red algae (RA) extracts. The pH of solution strongly influenced NP synthesis because changes in pH resulted in variation of their superficial charge and in their ability to bind metal cations. For gold and silver NPs, non-neutral pH increased NP synthesis (Makarov et al. 2013).

Estimates of NP size were obtained through dynamic light scattering (*dh*), and measure of ζ-potential: 65.68 nm and -20.83 mV for green algae and 111.73 nm and -31.66 mV for red algae, respectively. The average NPs dissolution has been estimated as 0.1-0.15%, which is consistent with previous analyses performed on CuO NPs (Marmiroli et al. 2021).

From the raw extracts of both GA and RA, at the end of the microwave-assisted process the yield was 0.52 g; after pyrolysis, the produced NPs resulted in 0.15 g and 0.19 g from GA and RA, respectively. The post pyrolysis yields of CuO NPs were 42.1% and 36.5% based on the amount of extract, from GA and RA respectively. There was no substantial difference in the yields of CuO NPs produced from extracts of either of the two different macroalgae.

 doi:10.20944/preprints202406.0774.v1

2.2. XRD Nanoparticle Characterization

X-Rays Powder Diffraction (PXRD) analysis resulted in equal diffractograms for the nanoparticles from the two types of algae. According to the Inorganic Crystal Structure Database (ICSD, card no. 92364) the NPs are composed of tenorite, and the dimensions could be estimated within the range of 30-40 nm for both nanoparticles deriving from red and green algae (Figure 1). The XRD diffractometry of CuO nanoparticles from *Halymenia dilatata* seaweed aqueous extract is slightly different, probably due to a capping agent formed during the nanoparticle synthesis (Sivakumar et al., 2023).

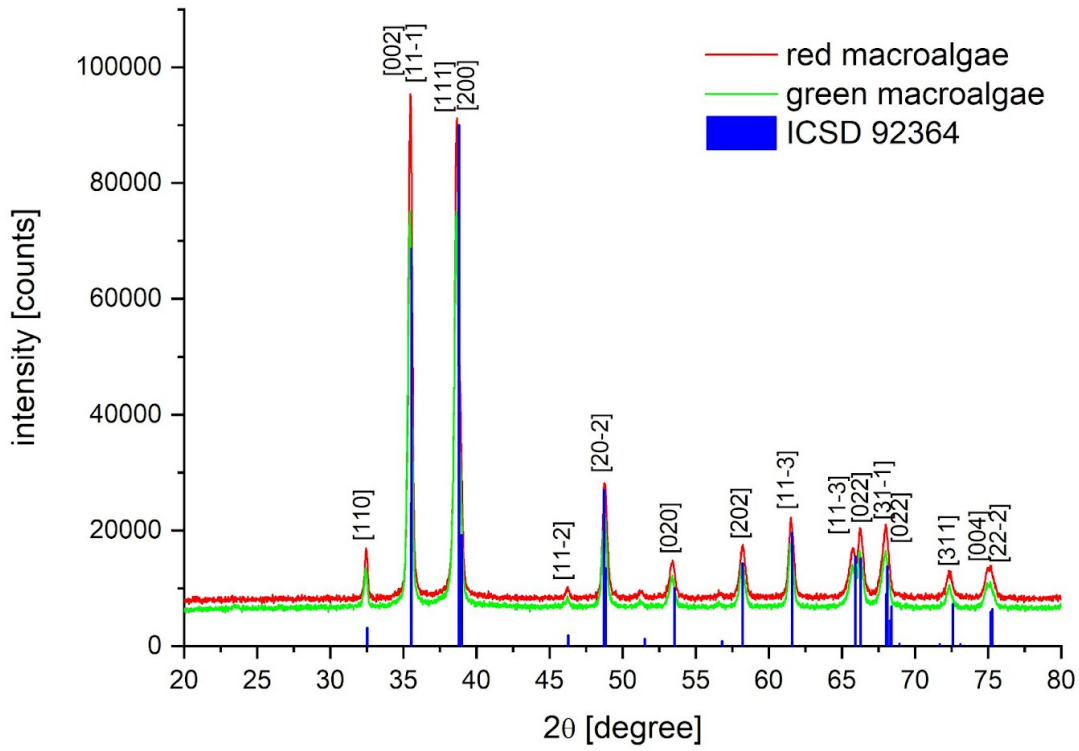

Figure 1. Diffractograms of the nanoparticles produced from the two macroalgae.

2.3. HR TEM/EDX

The images from the Talos HR-TEM (Figure 2) allowed us to observe single nanoparticles and the aggregates in which the crystal levels are visible. The aggregation dimension and the size and shape of both types of nanoparticles were quite similar and appeared to be around 30 nm with an ovoidal/round shape. The same shape and dimension are reported in the literature for the CuO NPs obtained from *Sargassum longifolium* using a similar green synthesis procedure (Rajeshkumar et al., 2021). The X-ray spectra from the two types of nanoparticles show the K and L X-ray peaks of Cu, O, and other elements. In the analyses with the JEOL HR-TEM, the sample presents only crystalline grains, with very variable dimensions. The two images include 100 nm markers. Size estimation is hampered by the difficulty of observing particles individually (Figure 2).

 doi:10.20944/preprints202406.0774.v1

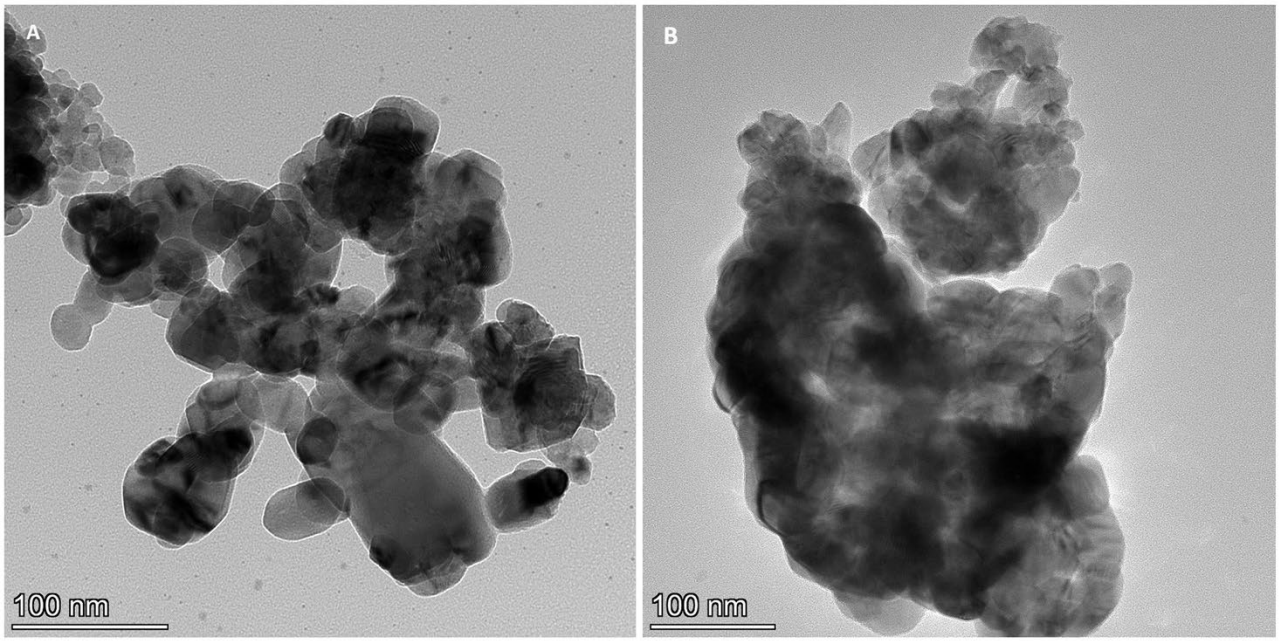

Figure 2. Nanoparticles from *U. lactuca* (A) and *G. verrucosa* (B).

The sample was dispersed on Ni lattices, to avoid confusing the response of the sample with that of the support. EDX measurements confirm the presence of only Cu and O in the samples (Figures 3 and 4); spurious signals in the spectrum represent the contribution of the analysis chamber.

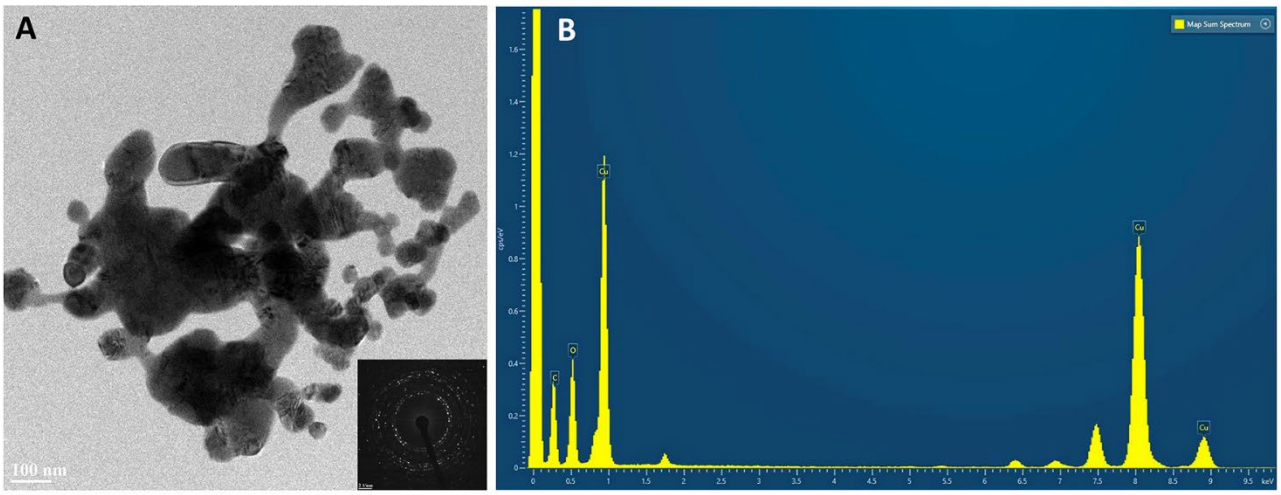

Figure 3. Nanoparticles from *G. verrucosa* (A) HR-TEM. (B) EDX.

 doi:10.20944/preprints202406.0774.v1

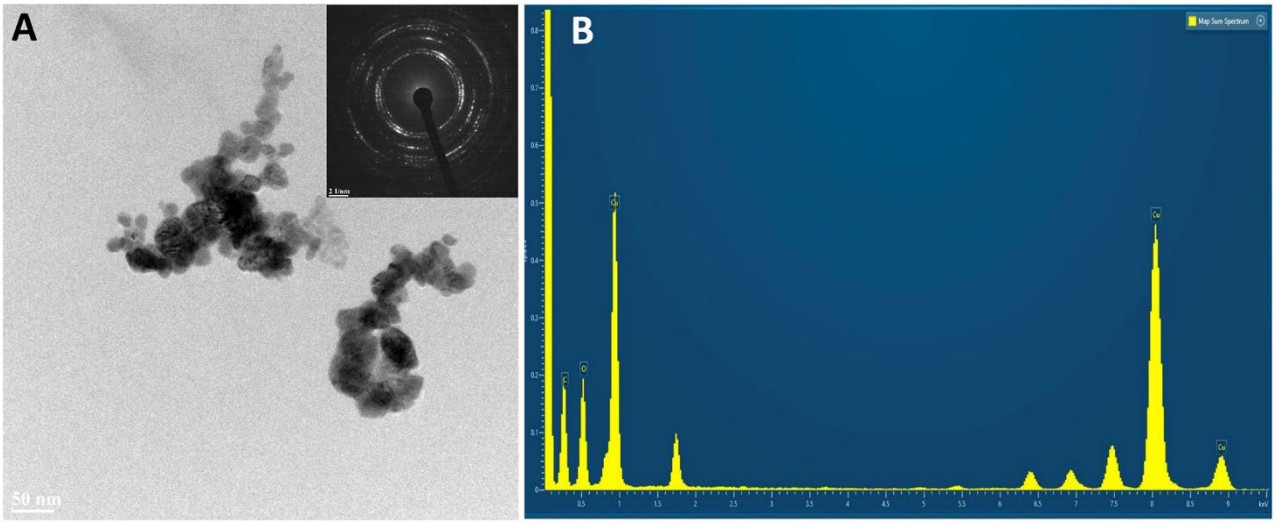

Figure 4. Nanoparticles from *U. lactuca* (A) HR-TEM. (B) EDX.

Samples from GA and RA also had grains with very variable sizes, as shown in Figures 3 and 4. The characteristics of the samples were that the individual crystals appear to be more agglomerated, as if they had partially 'sintered' (a word used here simply to indicate a greater interaction between the individual particles). On the left of Figure 2A we observed an agglomeration with particles that appear to be small, around 10-20 nm, but where the estimation of the size is even more difficult for the reason just described. The diffraction pattern confirms that only CuO is present, in agreement with the results of XRD.

2.4. FTIR Analyses

Before the heating treatment, FTIR analyses of CuO NPs were carried out to characterize the organic residue on the nanoparticles, to evaluate any differences in the organic functional groups derived from *U. lactuca* and *G. verrucosa.*

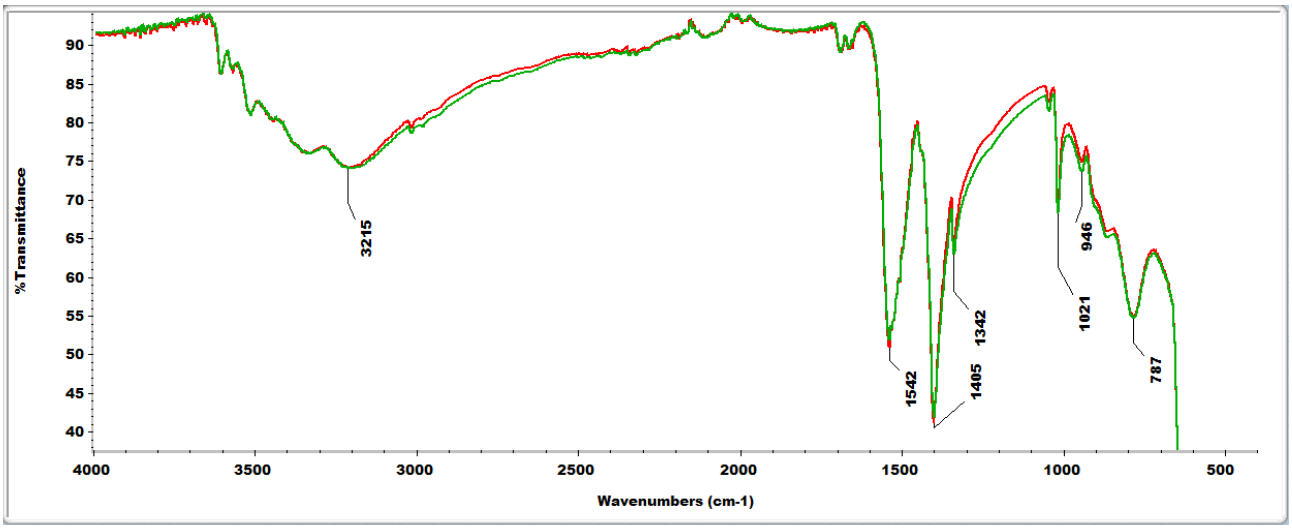

 doi:10.20944/preprints202406.0774.v1

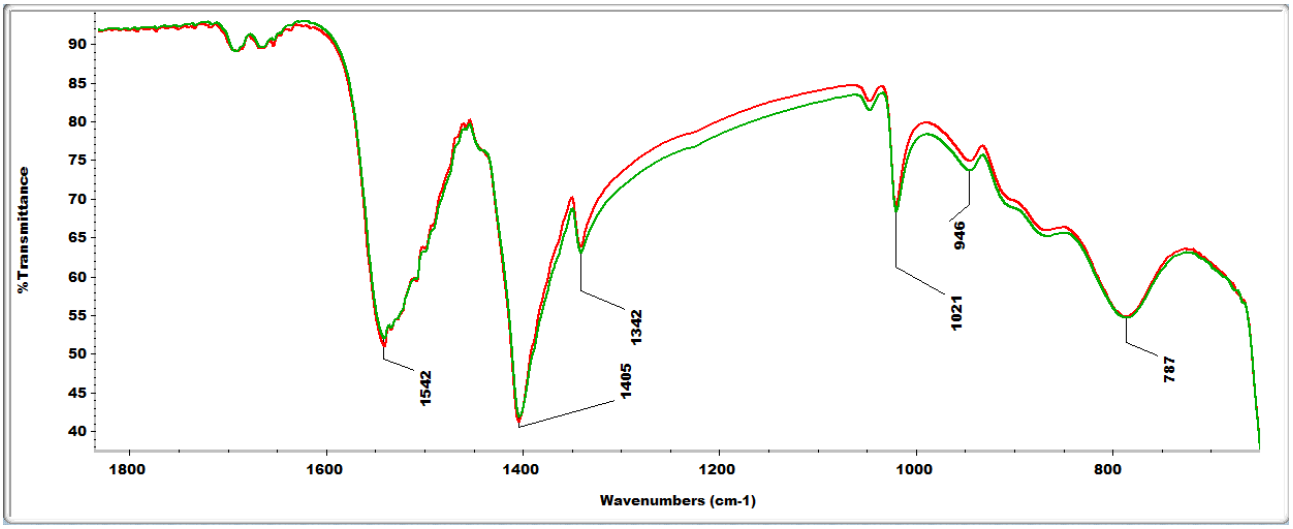

Figure 5. FTIR spectra of the nanoparticles derived from *U. lactuca* (green) and *G. verrucosa* (red), before the final heat treatment.

The two spectra are perfectly superimposable; the organic residues derived from the two different algae have the same composition. The FT-IR spectra are insufficient to identify the organic components. However, we can hypothesize the presence of some particular functional groups, basing on their known IR absorption (Coates 2000, Abidi 2021). The broad peak in the region 3500-3000 cm^{-1} can be seen as the result of multiple absorptions, such as those due to OH, NH and CH stretching; the peak at 1542 cm^{-1} could suggest the presence of aromatic rings (abundant for example in polyphenols), as it may be attributed to the aromatic ring stretch; the peak at 1405 cm^{-1} could be due to the bending of OH bonds; the peak at 787 cm^{-1} could be a further absorption of the aromatic rings.

2.4. Reactive Oxygen Species (ROS) Scavenging Capacity

The DPPH assay demonstrated that there is no difference in radical scavenging capacity between the nanoparticles obtained from the macroalgae and the standard CuO NPs (Figure 6). This means that the NPs obtained by algae behaved in the same way as the standards in the presence of ROS (Reactive oxygen species). Thus CuO NPs from macroalgae are able to quench the same amount of ROS as the standard CuO NPs.

 doi:10.20944/preprints202406.0774.v1

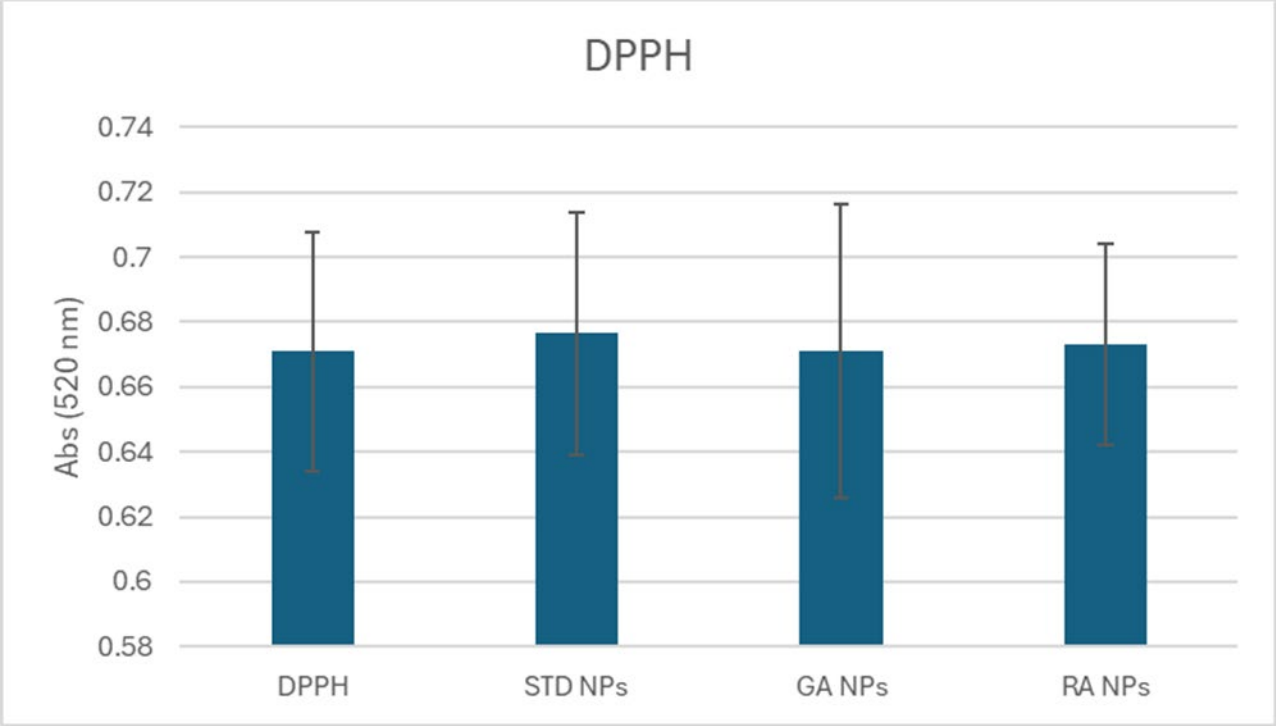

Figure 6. DPPH results for the nanoparticles from GA NPs and RA NPs in comparison with standard CuO NPs.

2.5. Microbiological Analysis on Copper Oxide (CuO) NPs

For the MIC (Minimum Inhibiting Concentration) determination, microbial cultures with OD_{600} = 0.05 were used and serial dilutions of CuO NPs were added to the cultures. The highest CuO NPs concentration under analysis was 500 mg/L and, from this, 10 serial dilutions (1:2) were performed. The microorganisms treated with nanoparticles, and the untreated control, were incubated at 28 °C for 24 h; then the OD_{600} was measured. The OD_{600} values measured for each microorganism after 24 h of CuO NPs treatment are reported in Tables 1-2 and Figures S1-S2. The NPs synthesized from macroalgae did not control any of the microorganisms except for *Escherichia coli*, which was inhibited by the nanoparticles from red algae at a concentration of 500 mg L^{-1}. This observation is confirmed by the fact that there is a reduction in respect to the control at 250 mg L^{-1}. When the microorganisms were treated with NPs from green or red algae there was a decrease in growth of at least 25% compared to the control, except for *Candida albicans*, which grew unchanged in this environment. This data, as in the case of *S. cerevisiae*, largely depends on the stability of the particle behavior in term of stability and aggregation, and subsequent bioavailability (Kasemets et al., 2009; Pagano et al. 2018). In particular, Kasemets et al., (2009) demonstrated how the cytotoxic effects of CuO NPs were mainly ascribed to Cu^{2+} ion release. This might depend on the medium utilized, and the dissociation rate may vary in respect to particle size and stability (Marmiroli et al., 2021). Flow cytometry analyses (Figure S3) on *C. albicans* and *S. cerevisiae* confirmed the different susceptibility of the two yeasts to the CuO NPs treatments. Differences observed can be ascribed to differences in cell wall permeability, since standard and biosynthesized CuO NPs were highly stable. The increase of cell mortality due to the treatment, particularly for *C. albicans*, suggested that a cytotoxicity effect was observed.

Table 1. Growth inhibition by NPs. STD, commercial product; GA, green algae NPs; RA, red algae NPs. A graphical representation is given in Figure S1.

	Candida albicans
	NPs concentration (mg L^{-1})

 doi:10.20944/preprints202406.0774.v1

	500	250	125	62.5	31.3	15.6	7.8	3.9	2.0	1.0	0.5	CTRL
STD NPs	1.098	1.233	1.31	1.342	1.349	1.335	1.333	1.361	1.364	1.377	1.372	1.341
GA NPs	1.092	1.259	1.326	1.363	1.362	1.367	1.386	1.393	1.382	1.383	1.391	1.343
RA NPs	1.11	1.304	1.363	1.383	1.374	1.398	1.407	1.387	1.399	1.393	1.396	1.407

	Saccharomyces cerevisiae											
	NPs concentration (mg L^{-1})											
	500	**250**	**125**	**62.5**	**31.3**	**15.6**	**7.8**	**3.9**	**2.0**	**1.0**	**0.5**	**CTRL**
STD NPs	0.915	1.021	1.111	1.13	1.218	1.141	1.246	1.249	1.248	1.249	1.206	1.114
GA NPs	0.863	0.982	1.079	1.177	1.158	1.191	1.226	1.253	1.235	1.283	1.314	1.231
RA NPs	0.831	1.013	1.129	1.127	1.2	1.233	1.248	1.304	1.304	1.334	1.375	1.354

	Bacillus subtilis											
	NPs concentration (mg L^{-1})											
	500	**250**	**125**	**62.5**	**31.3**	**15.6**	**7.8**	**3.9**	**2.0**	**1.0**	**0.5**	**CTRL**
STD NPs	0.05	0.05	0.05	0.11	0.634	0.921	0.965	0.996	0.965	1.025	0.995	0.997
GA NPs	0.566	0.856	0.921	0.985	1.005	1.025	1.008	1.013	1.007	0.966	0.975	0.999
RA NPs	0.613	0.811	0.892	0.964	0.984	1.014	1.037	0.998	1.029	1.028	1.022	1.053

	Escherichia coli											
	NPs concentration (mg L^{-1})											
	500	**250**	**125**	**62.5**	**31.3**	**15.6**	**7.8**	**3.9**	**2.0**	**1.0**	**0.5**	**CTRL**
STD NPs	0.605	0.711	0.72	0.723	0.725	0.722	0.716	0.712	0.703	0.716	0.721	0.662
GA NPs	0.402	0.564	0.644	0.673	0.713	0.703	0.673	0.672	0.657	0.678	0.666	0.66
RA NPs	0.05	0.074	0.52	0.706	0.737	0.732	0.695	0.698	0.675	0.695	0.7	0.705

	Staphylococcus aureus

 doi:10.20944/preprints202406.0774.v1

	NPs concentration (mg L^{-1})											
	500	**250**	**125**	**62.5**	**31.3**	**15.6**	**7.8**	**3.9**	**2.0**	**1.0**	**0.5**	**CTRL**
STD NPs	0.619	0.549	0.618	0.596	0.536	0.561	0.563	0.529	0.55	0.588	0.6	0.675
GA NPs	0.481	0.473	0.555	0.523	0.528	0.542	0.534	0.523	0.54	0.552	0.538	0.666
RA NPs	0.455	0.371	0.542	0.452	0.531	0.607	0.506	0.549	0.465	0.58	0.52	0.69

Table 2. Summary of the effects of the nanoparticles on microorganisms. STD, commercial product; GA, green algae NPs; RA, red algae NPs.

Growth inhibition (OD_{600} = 0.05)			
NPs concentrations (mg L^{-1})			
	STD NPs	GA NPs	RA NPs
Candida albicans	0	0	0
Saccharomyces cerevisiae	0	0	0
Bacillus subtilis	125.0	0	0
Escherichia coli	0	0	500.0
Staphylococcus aureus	0	0	0
50% growth reduction compared to the untreated control			
NPs concentrations (mg L^{-1})			
	STD NPs	GA NPs	RA NPs
Candida albicans	0	0	0
Saccharomyces cerevisiae	0	0	0
Bacillus subtilis	62.5	0	0
Escherichia coli	0	0	250.0
Staphylococcus aureus	0	0	0
25% growth reduction compared to the untreated control			
NPs concentrations (mg L^{-1})			
	STD NPs	GA NPs	RA NPs
Candida albicans	0	0	0
Saccharomyces cerevisiae	0	500	250.0

 doi:10.20944/preprints202406.0774.v1

Bacillus subtilis	31.25	500	500.0
Escherichia coli	0	500	125.0
Staphylococcus aureus	0	500	250.0

From the spot assay (Figures 7 and S2) it is evident that the CuO NPs from Green and Red macroalgae behave in a similar way in inhibiting the growth of the microorganisms in liquid media, where the bioavailability is higher. They inhibit only the growth of *Escherichia coli*, but not that of the other microorganisms at any concentrations. Also, the standard NPs do not inhibit the growth of *Candida albicans* or any other microorganism. Differently from our results, the CuO nanoparticles obtained from *Halymenia dilatate* by Sivakumar et al. (2023) were most effective against *Bacillus subtilis* and *Staphylococcus aureus*. Thus the different types of algae used to prepare the CuO NPs have an influence on their biological properties. Similarly, Wang et al. (2018) reported that CuO NPs obtained by green synthesis were found to have a potential antibacterial effect against *E. coli*; they did not screen other microorganisms. No inhibitory effects on growth were observed in solid media. This result can be ascribed to the limited dissolution of the CuO NPs utilized and to their limited bioavailability in solid media.

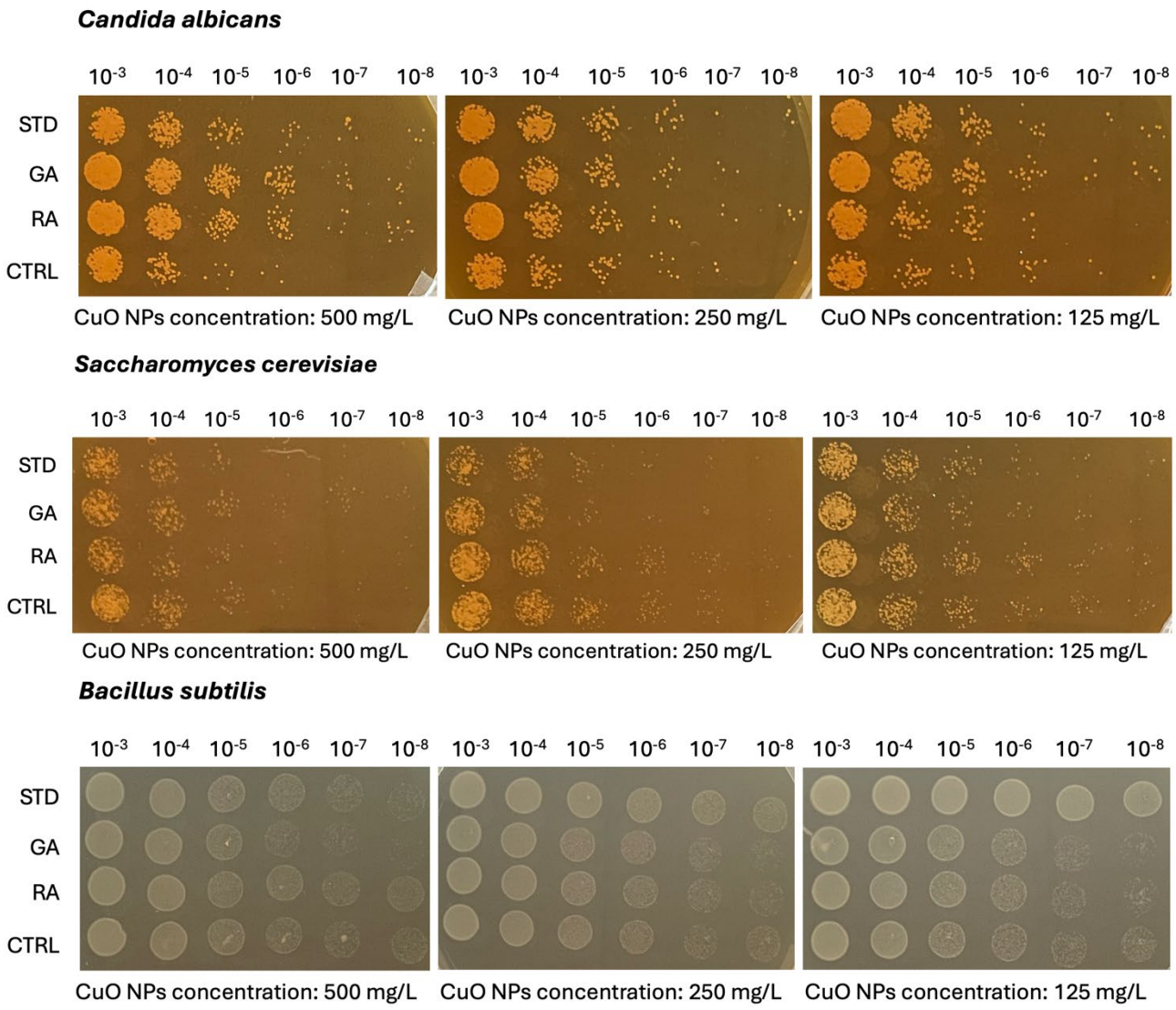

 doi:10.20944/preprints202406.0774.v1

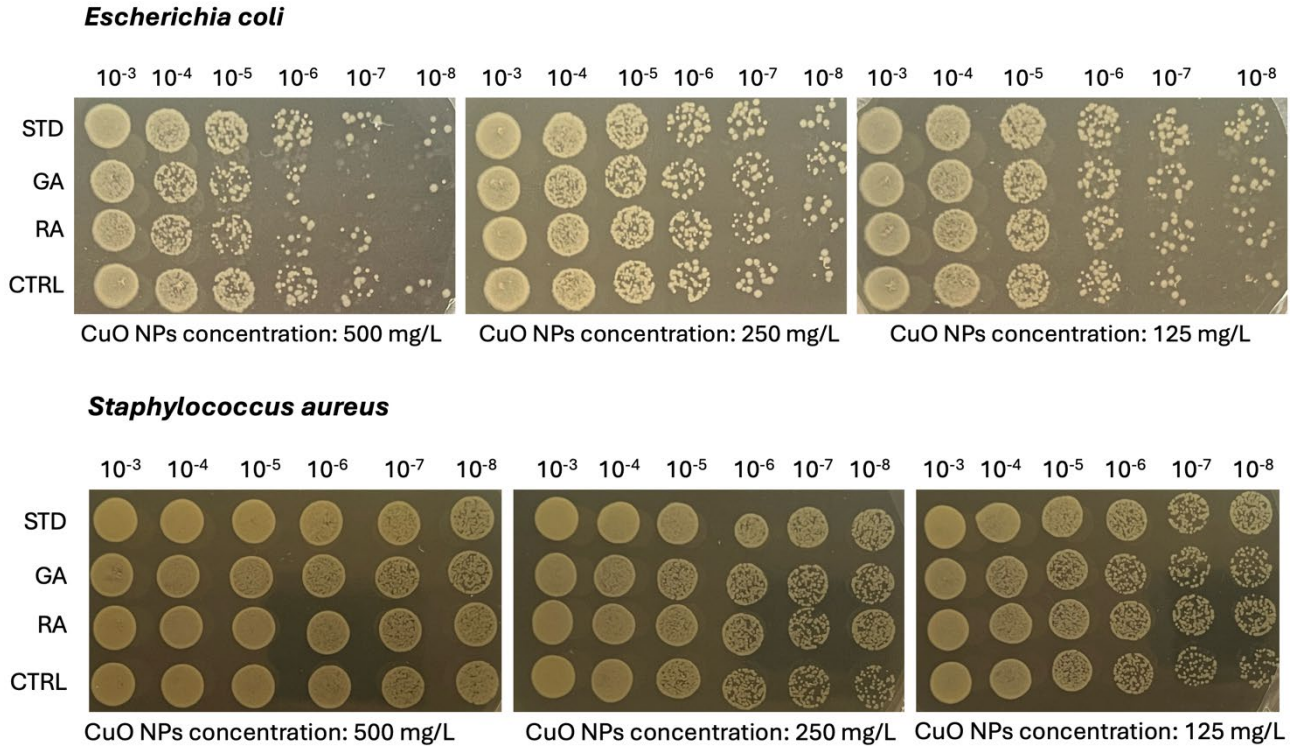

Figure 7. Spot assay of serial dilutions (from 10^{-3} to 10^{-8} cells mL^{-1}) of microorganisms treated in liquid media with CuO NPs. STD: standard CuO NPs, GA: CuO NPs synthesized from green algae, RA: CuO NPs synthesized from red algae, CTRL: untreated microorganisms. Ten µL of cell culture were plated on agar media after 24 h of incubation at 28 °C with the various NPs.

3. Materials and Methods

3.1. Macroalgae Biomass Collection and Extraction Process

Biomass from Green (*Ulva lactuca* L.) and red (*Gracilaria verrucosa* (H.) Papenfuss) macroalgae was collected in Sacca di Goro (Italy) in October 2023. Detailed descriptions of the two types of macroalgae utilized are reported in Dominguez & Loret, (2019) and Fredericq & Hommersand, (1989), respectively. Green and red macroalgae biomasses were washed at the site with seawater and immediately brought to the laboratory, where they were manually washed with tap water, then divided to obtain two different samples of both green and red biomass. Macroalgae were finally washed again three times with distilled water.

Biomasses were dried at room temperature for seven days (Figure S3) and grinded using a Kenwood Chopper CHP61. Macroalgae extraction was performed using the methods of Fatima et al. (2020) and Jayarambabu et al. (2020). Macroalgae extract was obtained with a biomass:ethanol 1:30 ratio on a hot-plate at 70 °C, under magnetic stirring (750 rpm), for 4 h. At the end, sonication was performed using Scientific Model 505 Sonic Dismembrator (Fisher Scientific, Waltham, MA) at 40% amplitude for 60 s to maximize dispersion. The extract was collected using centrifugation at 13000 rpm for 5 minutes, 4°C, and stored as the ethanol solution at 4 °C before NP synthesis.

3.2. NPs Synthesis

Cu-NPs synthesis was carried out following a modified version of the methodology of Jayarambabu et al. (2020). Copper acetate (Merck, Darmstadt, Germany) solution 0.1 M was added to macroalgae extract at 1:2 v/v ratio. Synthesis was performed by a microwave-assisted method. The mixed solution of copper acetate and microalgae extract was held for 30 seconds in a microwave oven at 600 W power; this operation was repeated 8 times. The synthesis of raw Cu-NPs was completed when the color of the solution changed from deep blue to light blue greenish (Figure S4). Isolation of

 doi:10.20944/preprints202406.0774.v1

raw NPs was performed using centrifugation at 13000 rpm for 5 minutes, 4°C; the pellet was dried at room temperature overnight. This pellet (Figure S5) was composed of copper oxide NPs and a precipitate of algal extract organic compounds.

The pellet was transferred into glass vials and dried at 80 °C in vacuum overnight to remove excess water. The temperature was then increased to 110 °C and maintained for 2 hours to remove final traces of water. The dry weight of the sample was noted and the FTIR spectra were acquired, before the heat treatment to decompose the organic matrix.

In the case of small batches, the sample was transferred into alumina vials and treated at 550 °C for 5 hours in a tubular furnace and oxygen/nitrogen atmosphere at a ratio of 1:5. For larger batches, a muffle mold was used, heated to the same temperature but performing the incineration in air. Interestingly, there were no appreciable differences using either approach for heat treatment, or on varying the heating curves. The samples were then collected and re-weighed to determine the weight loss due to the thermal treatment. CuO nanoparticles were obtained from both Green and Red Macroalgae, as verified with XRD and HR-TEM/EDX.

3.3. Nanoparticles Characterization

3.3.1. XRD

X-Rays Powder Diffraction (PXRD) analysis was performed to assess the structural properties of the obtained CuO NPs using a Rigaku Smartlab XE diffractometer in Bragg-Brentano geometry with Cu Kα wavelength (λ = 1.5406 Å) and a Ni filter to suppress the Kβ contribution; 5.0° Soller slits were used both on the incident and diffracted beam and data were collected using a HyPix3000 detector. Measurements were performed in the 10–80° 2θ range with 0.05 step size, acquiring in continuous 1D mode (2° min^{-1}).

All the observed reflections were indexed as belonging to monoclinic CuO (tenorite) according to the Inorganic Crystal Structure Database (ICSD, card no. 92364). Mean crystal size dimensions were calculated by pseudo-Voight fit and estimated to be within the 30 to 40 nm range. Notably, no spurious phases were observed (Figure 1).

3.3.2. HR TEM/EDX

We utilized initially a Talos high resolution TEM (Talos F200S G2, SEM FEG, Thermo Fisher Scientific, Waltham, MA, USA) equipped with an EDX detector. Nanoparticles were sonicated in Eppendorf tubes containing ethanol for 20 min, they were then spotted on Au TEM grids and allowed to evaporate for 15 minutes. We observed the morphology of single particles (Figure 2) and of aggregates, and took the EDX spectra at 80 KeV (Figure 2).

Then we verified the results obtained with the Talos TEM using a JEOL JEM2200FX field emission analytical Scanning-TEM microscope operated at 200 kV, equipped with two High Angle Annular Dark Field Detectors for Z contrast detection, a built-in W filter for Electron Energy Loss Spectroscopy, and an Oxford Aztec Energy TEM EDX system mounting the XPLORE Silicon Drift Detector with 80 mm^2 active area. The samples were dispersed on Nichel grids covered by continuous ultrathin carbon film (Figures 3, 4).

3.3.3. Zeta Potential, Particle Size and Dissolution

The average particle size (*dh*) and zeta (ζ) potential of the nanomaterials (100 mg L^{-1}) were determined in ddH_2O on a Zetasizer Nano Series ZS90 (Malvern Instruments, Malvern, UK), as described in Pagano et al. (2022). For particle suspension, CuO NPs for green and red algae (100 mg L^{-1}) were prepared in ddH_2O. Samples were collected after 1, 5, and 10 d. Aliquots of each sample (1 ml) were precipitated by ultracentrifugation at 30,000 rpm, for 10 min, at 20 °C (Optima Max-XP ultracentrifuge, Beckman−Coulter Inc., Brea, CA, USA). The liquid phase was collected and digested in 4 mL of 1 M HNO_3 (67% w/w) for 40 min at 200 °C using a VELP DK20 digester (VELP Scientifica, Usmate, Italy). Analysis was performed by flame atomic absorption spectroscopy (FA-AAS;

 doi:10.20944/preprints202406.0774.v1

AA240FS, Agilent Technologies, Santa Clara, CA, USA) for the presence of Cu (324.7 nm), as in Marmiroli et al. (2021).

3.3.4. FTIR

Infrared (IR) spectra were recorded with an Agilent Cary 630 FTIR spectrophotometer equipped with the attenuated total reflection (ATR) accessory (diamond), range 4000–650 cm^{-1}. For each sample, a small aliquot of dry powder was placed on the ATR system and tamped down, then the FT-IR spectrum was acquired directly (Figure 5).

3.3.5. DPPH Assay for Free Radical Scavenging Capacity

The 2,2-Diphenyl-1-picrylhydrazyl assay (DPPH assay) is a colorimetric method to measure the free radical scavenging activity of antioxidant compounds. According to Pagano et al. (2022), a solution of 0.06 mM DPPH in methanol was prepared daily. An aliquot of 50 µl of methanolic plant extract was added to 1.95 ml of DPPH solution; after 30 min at ambient temperature, the absorbance at 520 nm was measured (Varian Cary 50 spectrophotometer, Agilent Technologies). The absorbance was also read after 40 and 50 min of incubation to verify that a steady state was achieved (plateau in the curve). Appropriate solvent blanks were run in each assay (Figure 6).

3.3.6. Microbiological Analysis on Copper Oxide (CuO) Nanoparticles (NPs)

Five microorganisms were used: Saccharomyces cerevisiae BY4742, Candida albicans SC5314, Escherichia coli DH5α, Bacillus subtilis BV84, and Staphylococcus aureus ATCC 6538. C. albicans and S. cerevisiae were grown in YPD medium (yeast extract 1%, peptone 2%, dextrose 2%), while E. coli, B, subtilis and S. aureus were grown in Luria Bertani (LB) medium (yeast extract 0.5%, tryptone 1%, NaCl 1%). For each strain, a single colony was isolated from agar medium and cultured in LB and YPD broth for 24 h at 28 °C, with agitation. Then, OD_{600} was measured, and Minimal Inhibitory Concentration (MIC) determination was performed. Three different CuO NPs were used: standard (STD) NPs purchased from US Research Nanomaterials, Inc. (Houston, TX, USA) and previously characterized by Marmiroli et al. (2021), together with NPs synthesized from green algae and NPs synthesized from red algae.

For the MIC determination, microbial cultures with OD_{600} 0.05 were used and serial dilutions of CuO NPs were added to the cultures. The highest CuO NPs concentration under analysis was 500 mg L^{-1} and a further 10 serial dilutions (1:2) were performed. The microorganisms treated with nanoparticles, and the untreated control, were incubated at 28 °C for 24 h; then the OD_{600} was measured. The OD_{600} values obtained for each microorganism after 24 h of CuO NPs treatment are reported in Tables 1-2 and Figure S1. To better access the potential nanoparticle cytotoxic effects on the microorganisms under analysis, 10 µL of culture obtained from the three highest nanoparticles concentrations (500 mg L^{-1}, 250 mg L^{-1}, 125 mg L^{-1}) were plated on Petri dishes at 6 different cellular dilutions (10^{-3}-10^{-8}). The images of the spots obtained after 24 h of incubation at 28 °C are reported in Tables 1-2 and Figures 7, S2.

3.3.7. Flow Cytometry on Yeasts

S. cerevisiae and *C. albicans* strains were grown on liquid YPD for 24 h at 28 °C in the absence of NPs as control, or in the presence of 250 mg L^{-1} of each type of nanomaterial used (Standard, or green or red algae product). A total of 10^7 cells per each treatment were treated with propidium iodide (PI) as vital stain (5 µg mL^{-1}), for 20 min at 20°C. As an internal standard, a sample was included with induced 50% cell mortality, through thermal treatment at 100°C for 20 minutes. Samples were analyzed with an Attune NxT Flow Cytometer (Thermo Fisher Scientific, Wyman Street Waltham, MA, USA). Data were analyzed with Attune NxT software. A graph of the signal derived from PI analysis of cell mortality is reported in Figure S3.

4. Conclusions

 doi:10.20944/preprints202406.0774.v1

Macroalgae, especially *Ulva sativa* and *Glacilaria verrucosa*, are considered invading and noxious species by clam fishermen in the Northern Adriatic Sea in Italy. Every year this results in tons of macroalgae biomass being left to rot on the sand creating a foul odor. This causes problems for the clam fishermen, and is also detrimental for the tourism of the area. We have demonstrated that it is possible with green synthesis methods to obtain CuO nanoparticles of diameter 20-50 nm from biomass of these species. These nanoparticles are valuable because of their antimicrobial potential. Thus a marine nuisance can be converted to a useful material which may be exploited for human wellbeing.

Acknowledgments: The authors wish to thank Mirca Lazzaretti for assistance with flow cytometer.All the authors wish to thank: Funder: Project funded under the National Recovery and Resilience Plan (NRRP), Mission 4 Component 2 Investment 1.5—Call for tender No. 3277 of 30/12/2021 of Italian Ministry of University and Research funded by the European Union—NextGenerationEU Award Number: Project code ECS00000033, Concession Decree No. 1052 of 23/06/2022 adopted by the Italian Ministry of, CUP D93C22000460001, "Ecosystem for Sustainable Transition in Emilia-Romagna" (Ecosister).

References

1. Abid, N., Khan, A.M., Shujait, S., Chaudhary, K., Ikram, M., Imran, M., Haider, J., Khan, M., Khan, Q. et al. Synthesis of nanomaterials using various top-down and bottom-up approaches, influencing factors, advantages, and disadvantages: A review. Advances in Colloid and Interface. 2022, 18, 156-166.
2. Abidi, N. FTIR Microspectroscopy Selected Emerging Applications, Springer Nature Switzerland AG 2021, ISBN 978-3-030-84424-0.
3. Barciela, P., Carpena, M., Li, N.Y., Liu, C., Jafari, S.M., Simal-Gandara, J., Prieto, M.A. Macroalgae as biofactories of metal nanoparticles; biosynthesis and food applications. Advances in Colloid and Interface Science 2023, 311, 102829.
4. Castro, L., Blázquez, M.L., Muñoz, J.A., González, F., Ballester, A. Biological synthesis of metallic nanoparticles using algae. IET Nanobiotechnology, 2013, 7, 109–116.
5. Chatterjee, A., Kwatra, N., Abraham, J. Chapter 8— Challenges and Prospects Micro and Nano Technologies 2020, 143-157.
6. Chellapandian, C., Ramkumar, B., Puja, P., Shanmuganathan, R., Pugazhendhi, A., Kumar, P. Gold nanoparticles using red seaweed Gracilaria verrucosa: Green synthesis, characterization and biocompatibility studies, Process Biochem. 2019, 80, 58–63.
7. Coates, J. Interpretation of Infrared Spectra, A Practical Approach, in Encyclopedia of Analytical Chemistry, R.A. Meyers (Ed.), 10815–10837, 2000, John Wiley & Sons Ltd., Chichester.
8. De Almeida, C.L.F., Falc˜ao, H.d.S., Lima, G.R.d.M., Montenegro, C.d.A., Lira, N.S., de Athayde-Filho, P.F., Rodrigues, L.C., De Souza, M.d.F.V., Barbosa-Filho, J.M., Batista, L.M. Bioactivities from Marine Algae of the Genus Gracilaria. Int. J. Mol. Sci. 2011, 12, 4550–4573.
9. De Oliveira, D.M.P.; Forde, B.M.; Kidd, T.J.; Harris, P.N.A.; Schembri, M.A.; Beatson, S.A.; Paterson, D.L.; Walker, M.J. Antimicrobial Resistance in ESKAPE Pathogens. Clin. Microbiol. Rev. 2020, 33, e00181-19.
10. Dominguez, H.; Loret, E.P. Ulva lactuca, A Source of Troubles and Potential Riches. Mar. Drugs 2019, 17, 357. doi: 10.3390/md17060357
11. EClinica Medicine. Antimicrobial Resistance: A Top Ten Global Public Health Threat. EClinical,Medicine, 2021, 41, 101221.
12. El-Seedi, H. R., El-Shabasy, R.M., Shaden, Khalifa, A. M., et al. Metal nanoparticles fabricated by green chemistry using natural extracts: biosynthesis, mechanisms,and applications. RSC Adv. 2019. 9, 24539.
13. Fatima, R., Priya, M., Indurthi, L., Radhakrishnan, V., Sudhakaran, R.Biosynthesis of silver nanoparticles using red algae Portieria hornemannii and its antibacterial activity against fish pathogens. Microbial Pathogenesis, 2020, 138, 103780.
14. Ficko-Blean, E., Hervé, C., Michel, G. Sweet and sour sugars from the sea: the biosynthesis and remodeling of sulfated cell wall polysaccharides from marine macroalgae. Perspectives in Phycology, 2015, 251–64.
15. Fredericq, S., Hommersand, M.H. Proposal of the Gracilariales ord. nov. (Rhodophyta) based on an analysis of the reproductive development of Gracilaria verrucosa. Journal of Phycology 1989, 25, 213–227, 57.
16. Gnanajobitha, G. Fruit-mediated synthesis of silver nanoparticles using Vitis vinifera and evaluation of their antimicrobial efficacy. Journal of Nanostructure in Chemistry, 2013, 3, 1–6.
17. Hu, J., Wang, Z., Li, J. Gold nanoparticles with special shapes: controlled synthesis, surface-enhanced Raman scattering, and the application in biodetection. Sensors. 2007. 7, 12, 3299–3311.

 doi:10.20944/preprints202406.0774.v1

18. Jayarambabu, N., Akshaykranth, A., Venkatappa Rao, T., Venkateswara Rao, K., Rakesh Kumar, R.Green synthesis of Cu nanoparticles using Curcuma longa extract and their application in antimicrobial activity. Materials Letters, 2020, 259, 126813.
19. Jin, R. Nanotechnology Reviews. The impacts of nanotechnology on catalysis by precious metal nanoparticles. 2012. 1, 1, 31–56.
20. Kasemets K., Ivask A., Dubourguier H.C., Kahru A., Toxicity of nanoparticles of ZnO, CuO and TiO2 to yeast Saccharomyces cerevisiae, Toxicology in Vitro, 2009, 23, 1116-1122.
21. Khalil, I.; Yehye,W.A.; Etxeberria, A.E.; Alhadi, A.A.; Dezfooli, S.M.; Julkapli, N.B.M.; Basirun,W.J.; Seyfoddin, A. Nanoantioxidants: Recent Trends in Antioxidant Delivery Applications. Antioxidants 2020, 9, 24.
22. Khan, I., Saeed, K., and Khan, I. Nanoparticles: Properties, applications and toxicities Arabian Journal of Chemistry. 2019. 12, 7, 908–931.
23. Kloareg, B., Badis, Y., Cock, J.M., Michel, G. Role and Evolution of the Extracellular Matrix in the Acquisition of Complex Multicellularity in Eukaryotes: A Macroalgal Perspective. Genes, 2021, 12, 1059-167.
24. Kumar, D. A., Palanichamy, V., and Roopan, S. M. Green synthesis of silver nanoparticles using Alternanthera dentata leaf extract at room temperature and their antimicrobial activity Spectrochimica Acta Part A: Molecular and Biomolecular Spectroscopy. 2014. 127, 168–171.
25. Makarov, M.V., Ryzhik, I.V., Voskoboinikov, G.M. The Effect of Fucus vesiculosus L. (Phaeophyceae) Depth of Vegetation in the Barents Sea (Russia) on Its Morphophysiological Parameters. International Journal on Algae, 2013. 15, 1, 77-90.
26. Mantri, V.A., Kavale, M.G., Kazi, M.A. Seaweed Biodiversity of India: Reviewing Current Knowledge to Identify Gaps, Challenges, and Opportunities. Diversity, 2019, 12 (1), 13.
27. Mariselvam, R., Ranjitsingh, A. J. A., Usha Raja Nanthini, A., Kalirajan, K., Padmalatha, C., Mosae., Selvakumar, P. Green synthesis of silver nanoparticles from the extract of the inflorescence of Cocos nucifera (Family: Arecaceae) for enhanced antibacterial activity Spectrochimica Acta Part A: Molecular and Biomolecular Spectroscopy, 2014.129, 537–541.
28. Marmiroli, M., Pagano, L., Rossi, R., De La Torre-Roche, R., Lepore, G.O., Ruotolo, R., Gariani, G., Bonanni, V., Pollastri, S., Puri, A., Gianoncelli, A., Aquilanti, G., d'Acapito, F., White, J.C., Marmiroli, N., Copper Oxide nanomaterial fate in plant tissue: nanoscale impacts on reproductive tissues. Environ. Sci. Technol. 2021, 55 (15), 10769–10783.
29. Mourdikoudis, S., Pallares, R. M., and Thanh N. T. K. Characterization techniques for nanoparticles: comparison and complementarity upon studying nanoparticle properties. Nanoscale, 2018, 10, 12871.
30. Mussin, J.; Giusiano, G. Biogenic silver nanoparticles as antifungal agents. Front. Chem. 2022, 10, 1023542.
31. Nath, D., Banerjee, P. Green nanotechnology–a new hope for medical biology. Toxicology and Pharmacology. 2013. 36, 3, 997–1014.
32. Pagano, L., Marmiroli, M., Villani, M., Magnani, J., Rossi, R., Zappettini, A., White, J.C., Marmiroli, N. Engineered nanomaterial exposure affects organelle genetic material replication in Arabidopsis thaliana. ACS Nano 2022, 16, 2249–2260.
33. Pagano, L., Maestri, E., Caldara, M., White, J.C., Marmiroli, N., Marmiroli, M. Engineered nanomaterial activity at the organelle level: Impacts on the chloroplasts and mitochondria. ACS Sustain. Chem. Eng. 2018, 6, 12562–12579.
34. Pappou, S.; Dardavila, M.M.; Savvidou, M.G.; Louli, V.; Magoulas, K.; Voutsas, E. Extraction of Bioactive Compounds from Ulva lactuca. Appl. Sci. 2022, 12, 2117.
35. Pearce, A.K., Wilks, T.R., Arno, M.C. et al. Synthesis and applications of anisotropic nanoparticles with precisely defined dimensions. Nat Rev Chem. 2021.5, 21–45.
36. Pereira, A.M.; Costa, A.D.; Dias, S.C.; Casal, M.; Machado, R. Production and Purification of Two Bioactive Antimicrobial Peptides Using a Two-Step Approach Involving an Elastin-Like Fusion Tag. Pharmaceuticals 2021, 14, 956.
37. Rajeshkumar S, Aboelfetoh EF, Balusamy SR, Ali D, Almarzoug MHA, Tesfaye JL, Krishnaraj R. Anticancer, Enhanced Antibacterial, and Free Radical Scavenging Potential of Fucoidan- (Fucus vesiculosus Source) Mediated Silver Nanoparticles. Oxid Med Cell Longev. 2021, 2021, 8511576.
38. Ray, B., Lahaye, M. Cell-wall polysaccharides from the marine green alga Ulva "rigida" (Ulvales, Chlorophyta). Chemical structure of ulvan. Carbohydrate Research, 1995, 274, 251–261.
39. Sangeetha, N., Saravanan, K. Biogenic silver nanoparticles using marine seaweed (Ulva lactuca) and evaluation of its antibacterial activity. Journal of Nanoscience and Nanotechnology. 2014, 2(1) 99-102.
40. Sivakumar S, Jin DX, Rathod R, Ross J, Cantley LC, Scaltriti M, Chen JW, Hutchinson KE, Wilson TR, Sokol ES, Vasan N. Genetic Heterogeneity and Tissue-specific Patterns of Tumors with Multiple PIK3CA Mutations. Clin Cancer Res. 2023, 29, 1125-1136.

 doi:10.20944/preprints202406.0774.v1

41. Singh A., Jain, D., Upadhyay, M.K., et al. Green synthesis of silver nanoparticles using Argemone mexicana leaf extract and evaluation of their antimicrobial activities. Digest Journal of Nanomaterials and Biostructures, 2010 .5, 2, 483–489,
42. Singaravelu, G., Arockiamary, J., Kumar, V.G., Govindaraju, K. A novel extracellular synthesis of monodisperse gold nanoparticles using marine alga, Sargassum wightii Greville. Colloids Surf. B Biointerfaces 2007, 57 (1), 97–101.
43. Suresh, A. K., Pelletier, D. A., Wang, W.et al., Ciprofloxacin functionalized biogenic gold nanoflowers as nanoantibiotics against pathogenic bacterial strains. Acta Biomaterialia, 2011. 7, 5, 2148–2152.
44. Thakkar, K.N., Mhatre, S.S., Parikh, R.Y. Biological synthesis of metallic nanoparticles. Nanomedicine: Nanotechnology, Biology and Medicine. 2010. 6, 2, 257–262.
45. Türk M., Erkey, C. Synthesis of supported nanoparticles in supercritical fluids by supercritical fluid reactive deposition: Current state, further perspectives and needs. The Journal of Supercritical Fluids, 2018. 134, 176–183.
46. Vestby, L.K.; Grønseth, T.; Simm, R.; Nesse, L.L. Bacterial Biofilm and its Role in the Pathogenesis of Disease. Antibiotics, 2020, 9, 59.
47. Viaroli, P., Azzoni, R., Bartoli, M., Giordani, G., Tajé, L. Evolution of the trophic conditions and dystrophic outbreaks in the Sacca di Goro lagoon; In: Northern Adri-atic Sea; In: Faranda, F.M., Guglielmo, L., Spezie G. (eds) Structure and processes in the Mediterranean ecosystems. Springer, Berlin Heidelberg New York, p 443.
48. World Health Organitation. Antimicrobial Resistance; WHO, Geneva, Switzerland, 2021
49. World Health Organization. Fungal Priority Pathogens List to Guide Research, Development and Public Health Action; WHO, Geneva, Switzerland, 2022.
50. Zhao J. and Stenzel M.H. Entry of nanoparticles into cells: The importance of nanoparticle properties. Polym. Chem., 2018,9, 259-272.
51. Zhang Y, Wang L, Xu X, Li F, Wu Q. Combined systems of different antibiotics with nano-CuO against Escherichia coli and the mechanisms involved. Nanomedicine (Lond). 2018, 13(3):339-351.
52. Zaldívar J.M., E. Cattaneo, M. Plus, C.N. Murray, G. Giordani, P. Viaroli. Long-term simulation of main biogeochemical events in a coastal lagoon: Sacca Di Goro (Northern Adriatic Coast, Italy). Continental Shelf Research 2003, 23, 1847–1875.
53. Zulfiqar, H., Zafar, A., Rasheed, M.N., Ali, Z., Mehmood, K., Mazher, A., Hasan, M., Mahmood, N. Synthesis of silver nanoparticles using Fagonia cretica and their antimicrobial activities. Nanoscale Adv. 2018 4;1(5):1707-1713.